MODELLING OF FLIGHT DYNAMICS
OF AN AIRPLANE ENCOUNTERING TRAILING VORTICES
GENERATED BY ANOTHER AIRPLANE

Bogusław Czechowicz

Air Force Institute of Technology
Księcia Bolesława Street 6, 01-494 Warsaw, Poland
tel./fax: +48 22 685 10 13
e-mail: boguslaw.czechowicz@itwl.pl

Grzegorz Kowaleczko

Air Force Academy and Air Force Institute of Technology
Księcia Bolesława Street 6, 01-494 Warsaw, Poland
tel.:+48 22 6851191
e-mail: g.kowaleczko@chello.pl

Mirosław Nowakowski

Air Force Institute of Technology
Księcia Bolesława Street 6, 01-494 Warsaw, Poland
e-mail: mmiroslaw.nowakowski@itwl.pl

Abstract

This paper presents method of flight dynamics modelling for aircraft encountering trailing vortices generated by other airplane. The mathematical model of 6-DOF spatial motion was applied. Aerodynamic forces produced by a wing were calculated using strip theory method – the wing was divided into a series of chordwise strips and contribution of each strip in these forces was determined. Local angle of attack for each strip was determined taking into account an influence of trailing vortices. Exemplary results of simulations for the case of two straight vortices encountered by aircraft are shown. Incremental contributions to aerodynamic forces and moments of all strips are summed.

Model and description of trailing vortices, induced velocity inside the vortex, induced velocity outside the vortex, model of motion dynamics, equations of motion, airplane forces, moments acting on the airplane, aerodynamic forces and moments, trailing vortex effect on the airplane are presented in the paper.

In particular, pair of straight trailing vortices, induced velocity for Rankine vortex, strip model of the wing, angle of attack for the strip, airplane pitch angle, bank angle, altitude, trajectory are illustrated

Keywords: air transport, airplane, airplane flight dynamics, trailing vortices

1. Introduction

A wing of flying aircraft leaves a vortex sheet, which rapidly wraps into a pair of contra-rotating vortices [2, 6]. This vortex field is hazardous for other airplanes during landing approach or take off. An influence of vortices on following aircraft depends on circulation of trailing vortices. This circulation grows for increasing mass of vortex-generating aircraft and it is inversely proportional to its velocity. Therefore vortices produced by large heavy airplanes flying slowly at high angles of attack are more hazardous, particularly during landing approach and take off phase [10]. To avoid such wake-vortex encounters followed aircraft must maintain a safe distance from a vortex-produced airplane up ahead of them. Including a size of the following aircraft the

separation limits for selected combinations of leader and follower airplanes have been determined by International Civil Aviation Organization [6].

The hazard also depends on the encounter direction. When the path of flight is perpendicular to the trailing vortices the significant impulse structural loads are observed. This is the result of changes of induced velocity direction which influences on an angle of attack.

If the path of the following aircraft is parallel to the pair of vortex this aircraft can experience overpowering rolling moments, reduction in its rate of climb (for a climbing aircraft) or an increased rate of descent (for a descending aircraft). This phenomenon is especially dangerous near the ground at landing phase of at flight when there is little altitude for recovery. The uncontrollable rolling moment is a result of asymmetry of flow around left and right wings.

Since induced velocity in a selected strip of wing is a function of its distance from vortices, therefore this velocity varies along the wing. Standard model of airplane motion dynamics does not allow taking this phenomenon into consideration – in this model, aerodynamic forces and moments are determined assuming that the angle of attack is the same for the whole airplane. Therefore different method of calculations should be used. The aerodynamic effect of the wake on the encountering airplane is determined using a strip theory method [13]. In this theory the wing is divided into a series of chordwise strips. Each strip is treated as a two-dimensional airfoil for which the incidence is determined taking into account the additional induced flow generated by vortices. Finally incremental contributions to aerodynamic forces and moments of all strips are summed.
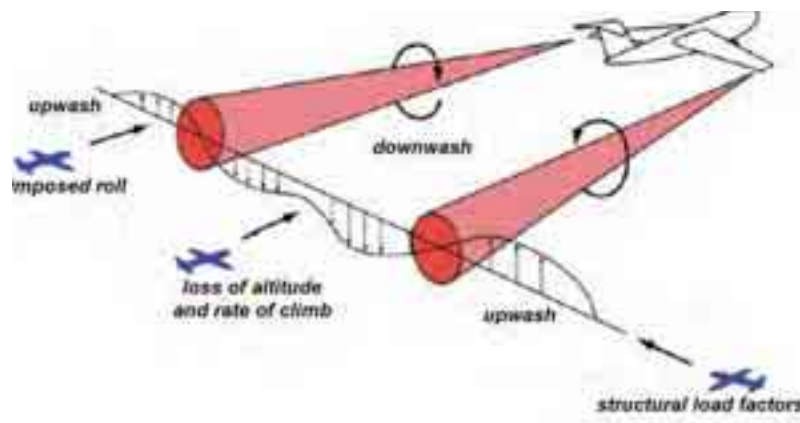

Fig. 1. Possible vortex encounters [3]

2. Model of Trailing Vortices

2.1. Trailing vortices description

The wing of flying airplane generates aerodynamic lift by creating a region of lower air pressure above it. Therefore the air from the high pressure region below the wing tends to migrate toward the top of the wing via the wingtips in a circular fashion. This starts the wake vortex. The difference of pressure between upper and lower surface of wing generates also small trailing edge vortices formed by outward and inward moving airstreams meeting at the trailing edge. In about five seconds in the distance of a few wing spans, all these vortices form pair of counter-rotating vortices. A structure of vortices is weakly unstable. At the beginning two straight vortices are observed. Next they are wavy and the waviness grows as a result of natural instability and finally the vortices from the left and right wings touch at different points along their length [11, 12]. They link together at these points and a series of vortex rings are produced. The lifespan of vortices is about three minutes and it depends on a few factors: atmospheric stability, wing strength and direction, mechanical turbulence and ground effect [1, 3, 8].

The circulation of trailing vortices decreases in time – it means that the pair of straight vortices has the most dangerous influence on the following airplane. Therefore this kind of vortices form is taken into consideration in this work.

2.2. Vortex model

There can be found a lot of various mathematical models of vortex in literature [6, 13], which are used to get an estimate of velocity induced at any point behind the vortex-generating aircraft. They are theoretical or are based on results of measures. The main difference between them is in description of changes of velocity in a transition region between a vortex core and an outer area. In our simulation the Rankine vortex model has been applied.

Induced velocity inside the vortex

In the Rankine model the vortex consists of a core, which rotates with constant angular velocity ω like a solid body containing constant circulation Γ_v and an outer potential flow free of vorticity. The vortex core radius r_c is in the range of 4–10 percent of wingspan. In the core area the induced velocity is equal to:

$$\mathbf{V}_{ind\_A} = \mathbf{\omega} \times \mathbf{r} = \frac{\Gamma_v}{2\pi r_c^2} \mathbf{1} \times \mathbf{r} , \tag{1}$$

where:
$\mathbf{1}$ – the unit vector parallel to the vortex axis,
$\mathbf{r}$ – vector determining position of point A in relation to the vortex.

Inside the straight vortex the induced velocity has only tangential component which is determined as follows:

$$V_\theta(r) = \frac{\Gamma_v}{2\pi r_c^2} r , \tag{2}$$

At the boundary of the vortex core this velocity is equal to:

$$V_\theta(r_v) = \frac{\Gamma_v}{2\pi r_c} . \tag{3}$$
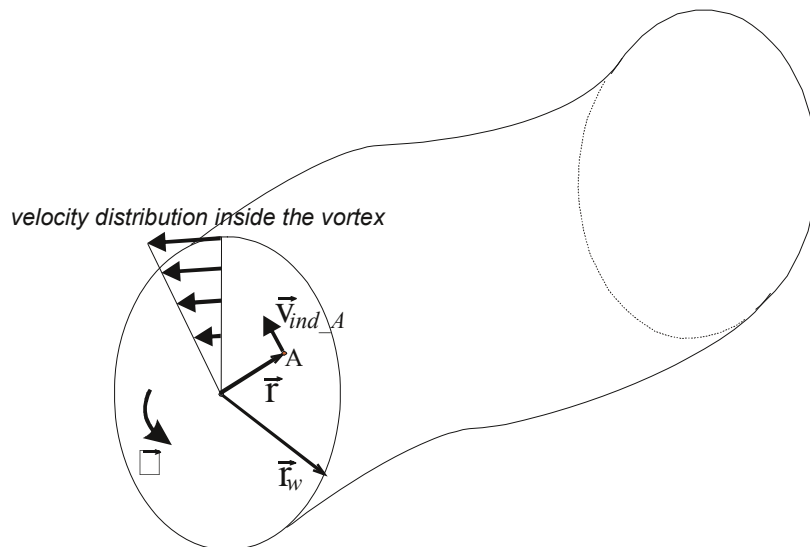

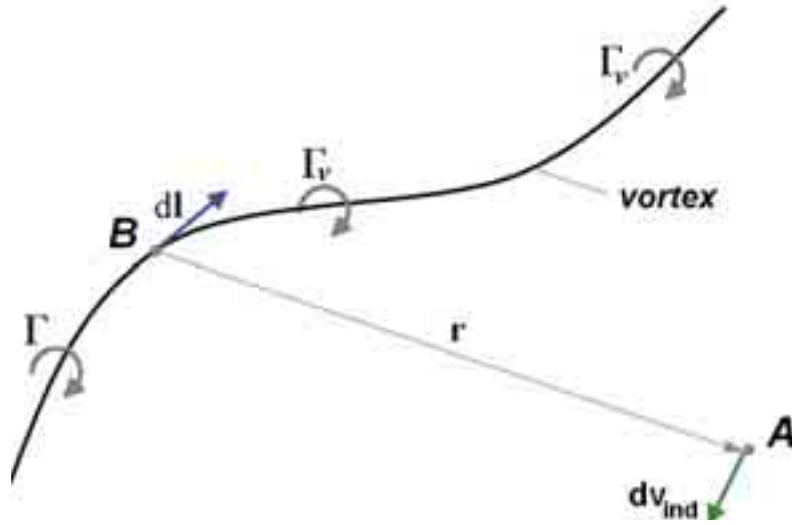*Fig. 2. Induced velocity inside the vortex*

Fig. 3. Induced velocity outside the vortex

Induced velocity outside the vortex

In the outer area the induced velocity $\mathbf{V}_{ind\_A}$ at a fixed point $A(r)$ can be calculated from the Biota-Savart law:

$$\mathbf{V}_{ind\_A} = \frac{1}{4\pi} \int_L \Gamma_v \frac{d\mathbf{l} \times \mathbf{r}}{|\mathbf{r}|^3} , \tag{4}$$

where $d\mathbf{l}$ is an element of the vortex filament, $\mathbf{r}$ is the position vector of the point A in relation to this element.

If the vortex is straight this integral may be calculated analytically. Using the vortex coordinate system $Ox_w y_w z_w$ shown in Fig. 4, the left vortex is given by $\Gamma_v = \Gamma$, $x_v = x_w$, $y_v = -b/2$, $z_v = 0$, and the right vortex is given by $\Gamma_v = -\Gamma$, $x_v = x_w$, $y_v = +b/2$, $z_v = 0$. We can obtain in $Ox_w y_w z_w$ two nonzero components of the induced velocity:

$$v_{ind\_A\_y_w} = -\frac{1}{2\pi} \sum \Gamma_v \frac{z_A}{(y_A - y_v)^2 + z_A^2} , \; v_{ind\_A\_z_w} = \frac{1}{2\pi} \sum \Gamma_v \frac{y_A - y_v}{(y_A - y_v)^2 + z_A^2} . \tag{5}$$

Figure 5 shows the exemplary course of the induced velocity obtained using Eqs (2) and (5) for one vortex. The sidewash and downwash velocities at the point A are obtained by summing the contributions of the left and right vortices:

$$v_{ind\_A\_y_w} = -\frac{1}{2\pi} \Gamma z_A \left[\frac{1}{\left(y_A + \dfrac{b}{2}\right)^2 + z_A^2} - \frac{1}{\left(y_A - \dfrac{b}{2}\right)^2 + z_A^2} \right] , \tag{5a}$$

$$v_{ind\_A\_z_w} = \frac{1}{2\pi} \Gamma \left[\frac{y_A + \dfrac{b}{2}}{\left(y_A + \dfrac{b}{2}\right)^2 + z_A^2} - \frac{y_A - \dfrac{b}{2}}{\left(y_A - \dfrac{b}{2}\right)^2 + z_A^2} \right] . \tag{5b}$$
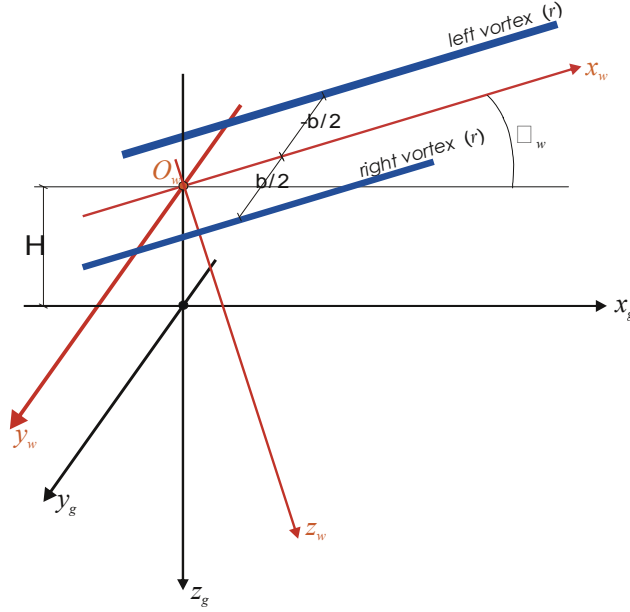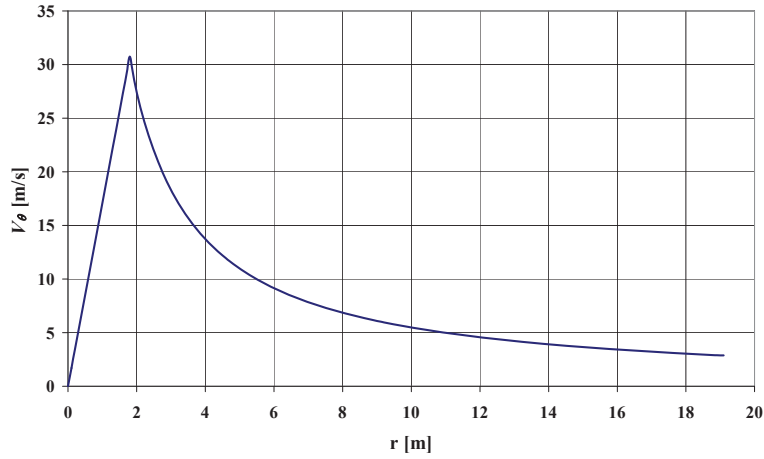
Fig. 4. Pair of straight trailing vortices

Fig. 5. Induced velocity for Rankine vortex

3. Model of Motion Dynamics

3.1. Equations of motion

Assuming that the airplane is a rigid body the spatial motion may be described using the Newton's second law:

$$\frac{d(m\mathbf{V})}{dt} = \sum_i \mathbf{F}_i , \quad \frac{d\mathbf{K}}{dt} = \sum_i \mathbf{M}_i ,$$ (6)

where:

m – the airplane mass,

$\mathbf{V}$ – the absolute translational velocity vector with components $[U, V, W]^T$ in the body axes *Oxyz*,

$\sum_i \mathbf{F}_i$ – the resultant of all the forces acting on m with components $[X, Y, Z]^T$,

$\mathbf{K}$ – the resultant angular momentum about the mass centre,

$\sum \mathbf{M}_i$ – the moment of external forces acting on the airplane with components $[L_\Sigma, M_\Sigma, N_\Sigma]^T$.

Equations (6) are complemented with kinematics relations and finally the set of twelve differential equations is determined:

Translational equations:

$$U = \frac{X}{m} - QW + RV ,$$
$$\dot{V} = \frac{Y}{m} - RU + PW , \tag{7}$$
$$\dot{W} = \frac{Z}{m} - PV + QU .$$

Rotational equations:

$$\dot{P} = \frac{1}{I_x I_z - I_{xz}^2}\left\{\left[L_\Sigma + (I_y - I_z)QR + I_{xz}PQ\right]I_z + \left[N_\Sigma + (I_x - I_y)PQ - I_{xz}QR\right]I_{xz}\right\},$$
$$Q = \frac{1}{I_y}\left[M_\Sigma + (I_z - I_x)RP + I_{xz}(R^2 - P^2)\right], \tag{8}$$
$$\dot{R} = \frac{1}{I_x I_z - I_{xz}^2}\left\{\left[L_\Sigma + (I_y - I_z)QR + I_{xz}PQ\right]I_{xz} + \left[N_\Sigma + (I_x - I_y)PQ - I_{xz}QR\right]I_x\right\}.$$

Kinematic equations:

$$\dot{\Phi} = P + (R\cos\Phi + Q\sin\Phi)\,tg\Theta ,$$
$$\dot{\Theta} = Q\cos\Phi - R\sin\Phi , \tag{9}$$
$$\dot{\Psi} = \frac{1}{\cos\Theta}(R\cos\Phi + Q\sin\Phi),$$

$$\dot{x}_g = U\cos\Theta\cos\Psi + V(\cos\Phi\sin\Psi - \sin\Phi\sin\Theta\cos\Psi) +$$
$$+ W(\cos\Phi\sin\Theta\cos\Psi + \sin\Phi\sin\Psi),$$
$$\dot{y}_g = U\cos\Theta\sin\Psi + V(\sin\Phi\sin\Theta\sin\Psi + \cos\Phi\cos\Psi) + \tag{10}$$
$$+ W(\cos\Phi\sin\Theta\sin\Psi - \sin\Phi\cos\Psi),$$
$$\dot{z}_g = -U\sin\Theta + V\sin\Phi\cos\Theta + W\cos\Phi\sin\Theta .$$

In these equations $\Omega = [P, Q, R]^T$ are airplane angular velocities relative to Earth in *Oxyz* system, $[\Theta, \Phi, \Psi]^T$ are the Euler angles of the airplane and $[x_g, y_g, z_g]^T$ give position of the airplane relative to $O_g x_g y_g z_g$ system (Fig. 5).
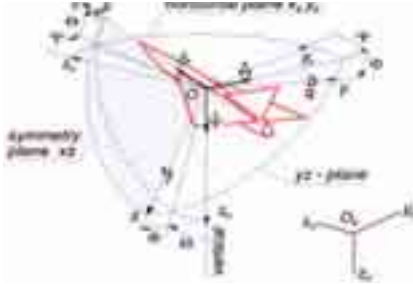

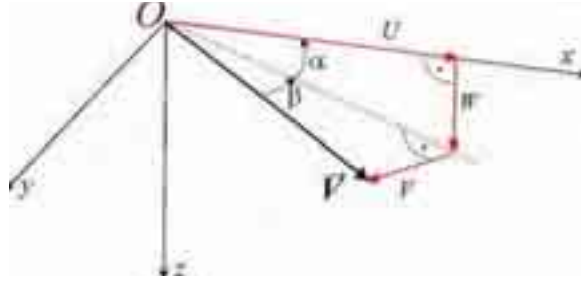*Fig. 5. Oxyz and $Ox_g y_g z_g$ coordinate systems*

Fig. 6. Angle of attack α and sideslip angle β

3.2. Airplane forces

The right hand side of the first equation of (6) represents forces acting on the airplane:

$$\mathbf{F} = \mathbf{Q} + \mathbf{R}_{aer} + \mathbf{T}, \tag{11}$$

where:
$\mathbf{Q}$ – the weight,
$\mathbf{T}$ – the trust,
$\mathbf{R}_{aer}$ – the aerodynamic force.

Components of these forces in the body axis system *Oxyz* are as follows:
1. the airplane weight Q:

$$Q_x = mg\sin\Theta, \quad Q_y = mg\cos\Theta\sin\Phi, \quad Q_z = mg\cos\Theta\cos\Phi, \tag{12}$$

2. the thrust T is parallel to the airplane longitudinal axis *Ox* and is equal to the thrust sum of left (*l*) and right (*r*) engines (it is assumed that the airplane is equipped with two engines mounted at left and right wings):

$$T_x = T_l + T_r, \quad T_y = 0, \quad T_z = 0, \tag{13}$$

3. the aerodynamic force R$_{aer}$:

$$R_x = \frac{\rho V^2}{2}S\left(-C_{xa}\cos\alpha\cos\beta - C_{ya}\cos\alpha\sin\beta + C_{za}\sin\alpha\right),$$

$$R_y = \frac{\rho V^2}{2}S\left(-C_{xa}\sin\beta + C_{ya}\cos\beta\right), \tag{14}$$

$$R_z = \frac{\rho V^2}{2}S\left(-C_{xa}\sin\alpha\cos\beta - C_{ya}\sin\alpha\sin\beta - C_{za}\cos\alpha\right),$$

where:
α – the angle of attack,
β – the sideslip angle (Fig. 6),
C_{xa}, C_{ya}, C_{za} – aerodynamic coefficients of drag, side force and lift,
S – the wing area,
ρ – the air density.

3.3. Moments acting on the airplane

Airplane rotation are forced by aerodynamic and gyroscopic moments and moments produced by engines. They are as follows:
1. the gyroscopic moments $\mathbf{M}_{gyr}$ is an effect of rotational motion of turbines:

$$\mathbf{M}_{gyr} = \sum_i J_i\boldsymbol{\omega}_i \times \boldsymbol{\Omega}, \tag{15}$$

where:
J_i – an inertia moment of *i*-th turbine,
$\boldsymbol{\omega}_i$ – an angular velocity of *i*-th turbine.
Its components in the body system *Oxyz* are:

$$L_{gyr} = 0, \quad M_{gyr} = -\left(J_l\omega_l + J_r\omega_r\right)R, \quad N_{gyr} = \left(J_l\omega_l + J_r\omega_r\right)Q, \tag{16}$$

2. the engine moments $\mathbf{M}_T$:

$$\mathbf{M}_T = \sum_i \mathbf{r}_{Ti} \times \mathbf{T}_i, \tag{17}$$

are determined taking into account locations of engines:

$$\mathbf{r}_{Tl} = [0,-y_T,0]^T, \quad \mathbf{r}_{Tr} = [0,y_T,0]^T. \tag{18}$$

Components of $\mathbf{M}_T$ in *Oxyz* are equal to:

$$L_T = 0, \quad M_T = 0, \quad N_T = \left(T_{left} - T_{right}\right)y_T, \tag{19}$$

3. the aerodynamic moment $\mathbf{M}_{aer}$ has following components in the body system:

$$L = C_l\frac{\rho V^2}{2}Sb_w, \quad M = C_m\frac{\rho V^2}{2}Sc_a, \quad N = C_n\frac{\rho V^2}{2}Sb_w, \tag{20}$$

where:
b_w – a wing span,

C_l, C_m, C_n – coefficients of rolling, pitching and yawing moments,

c_a – a mean aerodynamic chord.

3.4. Aerodynamic forces and moments

Aerodynamic coefficients were determined theoretically on the basis of engineering methods [4, 5, 7, 9] and the strip theory method [13]. Engineering methods were applied to calculate aerodynamic forces and moments produced by the fuselage and the tail. Formulas similar to (14) and (20) were used. For the wing the strip theory method was applied. Finally the resultant aerodynamic force of the whole aircraft was defined as:

$$\mathbf{R}_{aer} = \mathbf{R}_f + \mathbf{R}_w + \mathbf{R}_H + \mathbf{R}_V. \tag{21}$$

Subscripts denote: f – the fuselage, w – the wing, H – the horizontal tail, V – the vertical tail. Similar sum was for applied for resultant aerodynamic moments:

$$\mathbf{M}_{aer} = \mathbf{M}_f + \mathbf{M}_w + \mathbf{M}_H + \mathbf{M}_V. \tag{22}$$

Aerodynamic forces and moments of the wing are determined as the following integrals:

$$R_{xw} = \int_{wing} dR_x, \; R_{yw} = \int_{wing} dR_y, \; R_{zw} = \int_{wing} dR_z, \; L_w = \int_{wing} dL_w, \; M_w = \int_{wing} dM_w, \; N_w = \int_{wing} dN_w. \tag{23}$$

All integrals are calculated along the wing from $-b_w/2$ to $b_w/2$. There is necessary to determine a vector $\mathbf{r}_A = [\,x_A, y_A, z_A,]^T$ of the position of points A along the one-quarter-chord line. If y_A is the independent coordinate, then two other coordinates can be described as $x_A(y_A)$ and $z_A(y_A)$. The absolute velocity of the point A is:

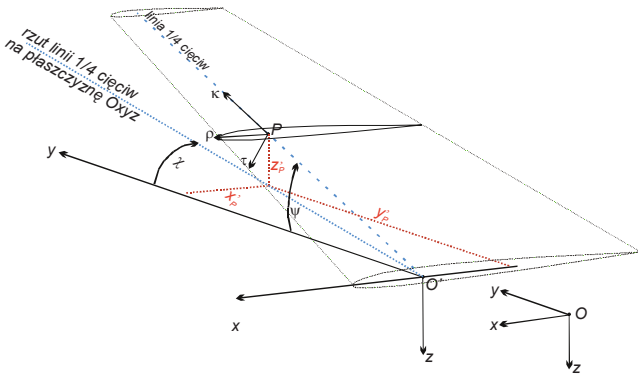$$\mathbf{V}_A = \mathbf{V} + \mathbf{\Omega} \times \mathbf{r}_A. \tag{24}$$
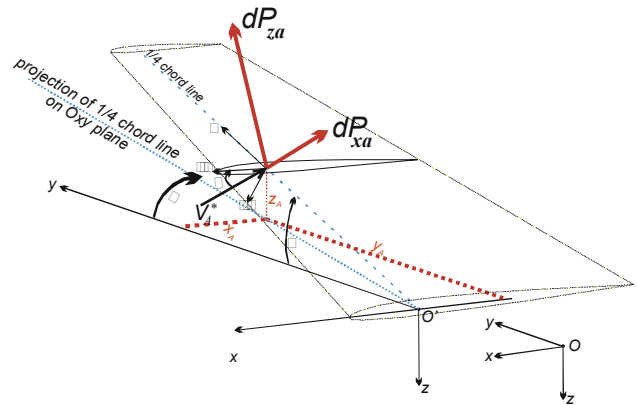

Fig. 7. Strip model of the wing

Fig. 8. Angle of attack for the strip

The difference between free-stream velocity and the induced velocity give the local velocity for the strip:

$$\mathbf{V}_A^* = \mathbf{V}_A - \mathbf{v}_{ind\_A}. \tag{25}$$

The strip angle of attack in a plane normal to the planform is then computed from:

$$\alpha_{st} = \arctan \frac{W_A^*}{U_A^*}, \tag{26}$$

where U_A^*, W_A^* are components of $\mathbf{V}_A^*$ in the local system of coordinates $A\rho\kappa\tau$ /Fig.7/.

The incremental aerodynamic forces of the strip determined in $A\rho\kappa\tau$ are:

$$dR_{\rho_a} = -dP_{xa} = -C_{xa\,st} \frac{\rho(V_A^*)^2}{2} c(\kappa) d\kappa, \; dR_{\tau_a} = -dP_{za} = -C_{za\,st} \frac{\rho(V_A^*)^2}{2} c(\kappa) d\kappa, \tag{27}$$

where $c(\kappa)$ is the chord of the strip, C_{xast}, C_{zast} are aerodynamic coefficients of the strip.

On the basis of Eqs (27) all integrals (23) can be calculated. For each strip transformation from the local coordinate system to the body axis system should be done.

4. Trailing Vortex Effect on the Airplane

The main goal of presented work is to determine the influence of trailing vortices on the encountering airplane. This dynamic response differs in time and depends on actual, relative to vortices, position of the following airplane. For the simulation purpose it is assumed that the pair of straight vortices are on horizontal plane. Trajectory of the airplane is straight and its orientation relative to vortices is described by two angles: Θ_t – the trajectory pitch angle and Ψ_t - the trajectory grazing angle. All these angles are shown in Fig. 9. Simulations have been done in ranges:

$$1^O \leq \Psi_t \leq 170^O \,,\, -30^O \leq \Theta_t \leq 30^O .$$
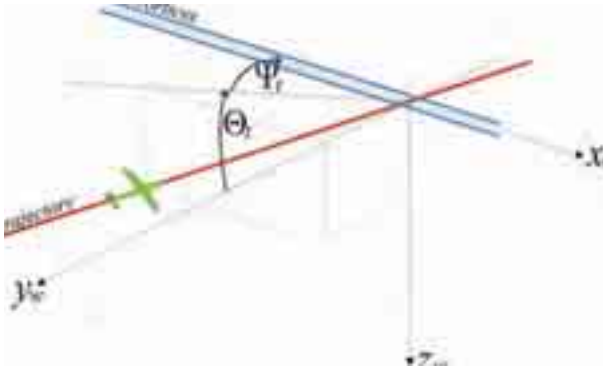
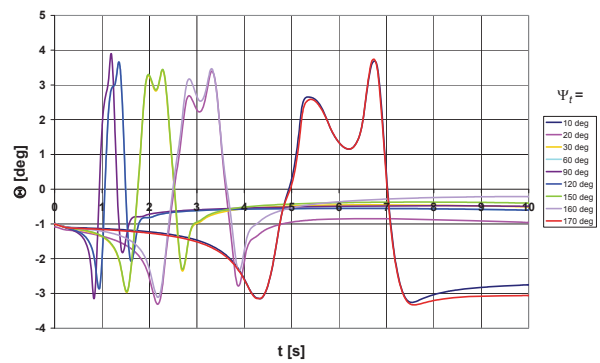

Fig. 9. Trajectory – vortices relative orientation

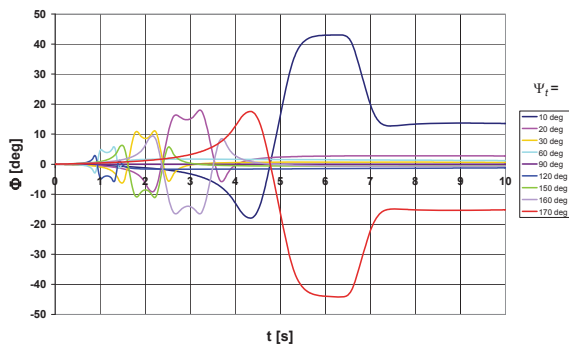Fig. 10. Airplane pitch angle Θ for level flight

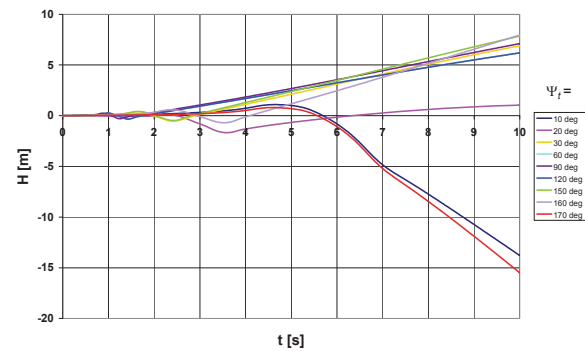Fig. 11. Airplane bank angle Φ for level flight
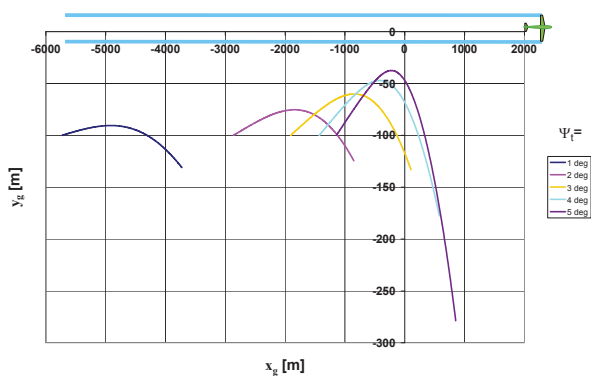

Fig. 12. Airplane altitude H for level flight

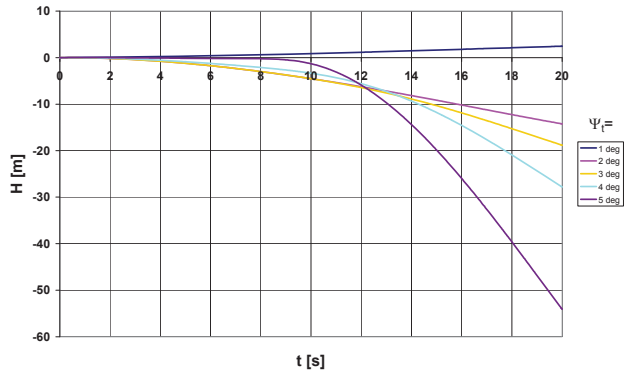Fig. 13. Airplane trajectory in boundary cases ($\Theta_t = 0^0$, $\Psi_t \leq 5^0$)

Fig. 14. Airplane altitude H in boundary cases ($\Theta_t = 0^0$, $\Psi_t \leq 5^0$)

49

Figure 10–12 present comprehensive courses of basic flight parameters for various grazing angles Ψ_t with the trajectory pitch angle Θ_t equal to zero. This means that the initial conditions are defined as steady level flight. Fig. 10 shows that the airplane pitch angle Θ is disturbed in the range of 7^0. More important are changes of the bank angle Φ (Fig. 11) - with decreasing grazing angle Ψ_t the bank angle grows up to 43^0. For small values of the grazing angle the altitude of the flight decreases Φ (Fig. 12). More detailed analysis shows that the boundary grazing angle Ψ_t can be determined. For this angle the plane is not able to fly across vortices and its trajectory is curved out of vortices. It is shown in Fig.13. In this case the altitude rapidly decreases (Fig.14).

Concluding remarks

The result of this preliminary study indicate that trailing vortices are potentially hazardous for other airplanes. Their influence on the motion of following aircraft depends on the configuration of vortices-trajectory system but the altitude and the maximum bank angle should be the hazard predominate criterion.

References

[1] Babie, B. M., Nelson, R. C., *An Experimental Study of Wake Vortex Instabilities*, Proceedings of 46th AIAA Aerospace Sciences Meeting and Exhibit, Reno 2008.
[2] Cotet, G. -H., Poncet P., *Simulation and Control of Three-Dimensional Wakes*, Computers and Fluids, Vol. 33, No. 5, pp. 697-713(17), 2004.
[3] Crow, S., Bate, E., *Lifespan of Trailing Vortices in a Turbulent Atmosphere*, Journal of Aircraft, Vol. 13, No. 7, 1976.
[4] Etkin, B., *Dynamics of Atmospheric Flight*, Johson Willey & Sons Inc., New York 1972.
[5] Finck, R., *USAF Stability and Control DAT*COM, Air Force Flight Dynamics Laboratory, Rep. No. AFWAL-TR-83-3048, 1978.
[6] Gertz, T., Holzapfel, F., Darracq, D., *Commercial Aircraft Vake Vortices*, Progress in Aerospace Science 38, pp. 181-208, 2002.
[7] Goraj, Z., *Dynamika i aerodynamika samolotów manewrowych z elementami obliczeń*, Biblioteka Naukowa Instytutu Lotnictwa, Warszawa 2001.
[8] Jacquin, L., Fabre, D., Sipp, D., Theofilif, V., Vollmers, H., *Instability and Unsteadiness of Aircraft Wake Vortices*, Aerospace Science and Technology, No. 7, pp. 577-593, 2003.
[9] Kowaleczko, G., *Zagadnienie odwrotne w dynamice lotu statków powietrznych*, Wydawnictwo Wojskowej Akademii Technicznej, Warszawa 2003.
[10] Nelson, R. C., *Trailing Vortex Wake Encounters at Altitude – A Potential Flight Safety,* AIAA Paper 2006-6268.
[11] Nelson, R. C., Babie, B. M., *An Experimental Study of the Stability of a Four-Vortex System*, AIAA Paper 2005-4852.
[12] Nelson, R. C., *The Trailing Vortex Wake Hazard: Beyond the Takeoff and Landing Coridors*, AIAA Paper 2004-5171.
[13] Reimer, H., Vicroy, D. D., *A Preliminary Study of a Wake Vortex Encounter Hazard Boundary for a B737-100 Airplane*, NASA TM 110223, 1996.